Transferred hyperfine fields in rare-earth-substituted YFe_2 and YNi_2

1994 J. Phys.: Condens. Matter 6 2385

(http://iopscience.iop.org/0953-8984/6/12/013)

J. Phys.: Condens. Matter 6 (1994) 2385–2394. Printed in the UK

Transferred hyperfine fields in rare-earth-substituted YFe_2 and YNi_2

Diana Guenzburger, R R Sobral and A P Guimarães

Centro Brasileiro de Pesquisas Físicas, Rue Xavier Sigaud 150, Urca, 22290-180 Rio de Janeiro, RJ, Brazil

Received 17 August 1993, in final form 9 November 1993

Abstract. In the intermetallic compound YFe_2, the metallic hyperfine field at the Y nucleus, as measured by ^{89}Y NMR spectroscopy, is affected by the substitution of one or more neighbour Y atoms by different rare-earth impurities. In order to understand the underlying mechanisms for the transferred hyperfine interaction, we have performed first-principles calculations, within the local spin-density theory, for embedded clusters representing a Y atom and its vicinity in the compounds $Y_{1-x}R_xFe_2$ (R = Gd, Tb, Ho, Tm or Lu) and $Y_{1-x}Gd_xNi_2$. The contact magnetic hyperfine field and the dipolar field were obtained; the resulting total field was found to increase with the spin of the rare-earth impurity. Orbital hyperfine fields were not considered. The contact transferred field was found to arise from direct polarization of the s electrons by the rare-earth spin.

1. Introduction

The rare earths form a large number of intermetallic compounds with the 3d transition elements [1]; they present very interesting magnetic properties, arising from the coexistence of localized and itinerant forms of magnetism. Among these compounds, the cubic Laves phases have attracted a good deal of attention; they allow the systematic study of magnetic properties of different rare-earth ions in the same high-symmetry metallic environment. Furthermore, many interesting magnetic effects may be expected from the interactions of f and d moments on the rare-earth and d moments on the transition-metal ions. Due to the fact that its valence electron configuration is similar to that of the lanthanides, Y is included in the group of the rare earths.

YFe_2 is an intermetallic compound of cubic Laves-phase crystal structure C15, which orders magnetically at 542 K [1]. Each Y atom is placed on a site of high symmetry ($\bar{4}3m$), and is surrounded by four other second-neighbour Y atoms. Previously, it was thought that the Y atoms in this compound were non-magnetic; it has now been established unambiguously, by experimental [2, 3] and theoretical [4–6] means, that Y carries a small 4d moment of its own, anti-parallel to the Fe 3d moment. The magnetic hyperfine (HF) field at the Y site in YFe_2 has been measured by nuclear magnetic resonance (NMR) of ^{89}Y, yielding a value of -220 kOe (the negative sign meaning a field anti-parallel to the magnetization) [7, 8]. On the other hand, YNi_2, with the same crystallographic structure, is known to be non-magnetic [1]. The pseudo-binary compounds of formula $(Y_{1-x}R_x)Fe_2$, where R is a rare earth, are formed with the same cubic crystal structure, the R atoms occupying the Y sites substitutionally.

In the $(Y_{1-x}R_x)Fe_2$ compounds, NMR measurements on ^{89}Y have shown a distribution of HF fields corresponding to different configurations of R neighbours; the HF fields in

0953-8984/94/122385+10$19.50

the neighbourhood of the rare-earth impurities increase in magnitude compared to the field in the pure Y compound [9]. This additional, or transferred, HF field is negative and amounts to a few kOe. Whether the increase in the Y hyperfine field induced by the rare earth is produced by direct polarization of the conduction electrons, or indirectly by d–d interactions involving the Fe atoms, is not established. The microscopic mechanisms leading to the magnetic behaviour of these pseudo-binary compounds can only be investigated by first-principles electronic-structure calculations.

We present results of electronic-structure calculations for embedded clusters representing rare-earth-substituted YFe_2. The lanthanides considered were Gd, Tb, Ho, Tm and Lu, and the numbers of R atoms in the clusters were chosen to simulate configurations of low and high local concentrations of neighbours. Furthermore, clusters representing YNi_2 with Gd substituting for Y were also considered; since this last compound is non-magnetic when pure, a comparison with the results for Gd-substituted YFe_2 would throw light on the role played by the coupling with the Fe magnetic moments.

The method employed was the first-principles discrete variational method (DVM) [10, 11], in the framework of density functional theory and the local spin-density approximation (LSDA). The clusters of atoms representing the solid are embedded in the potential of several layers of external atoms; the Madelung potential is also taken into account. This method has been proven to be useful in deriving and understanding the magnetic and hyperfine properties of quite a number of metals and alloys. Among others, magnetic moments and hyperfine fields of Fe–Ni [12, 13] and Fe–Al [14] alloys were investigated, as well as local moments of impurities in s–p [15, 16] and transition metals [17, 18]. The atomic cluster representation of the solids is adequate, inasmuch as local properties are being investigated. As mentioned earlier, ^{89}Y NMR spectra of $(Y_{1-x}R_x)Fe_2$ discriminate between different configurations of R neighbours of Y [9, 19, 20]; similar studies on the pseudo-binary compounds $Y(Fe_{1-x}A_x)_2$ (A = Co, Al, Pt) show well resolved satellite structures of the Y resonance [21]. These results indicate that the Y hyperfine field is strongly affected by the interactions with the nearest magnetic neighbour atoms, this being a further indication of the adequacy of the embedded-cluster approach.

This paper is organized as follows: in section 2, the theoretical method is briefly described; in section 3, the analysis of the experimental data is presented; in section 4, calculated values of magnetic moments, spin densities and Y hyperfine fields are presented and discussed, and the latter are correlated to the experimental data. In section 5 we summarize our conclusions.

2. Theoretical method

The method employed was the discrete variational method (DVM) [10, 11], based on density functional theory and the local spin-density (LSD) approximation (see for example [22]). The solids are represented by clusters of atoms, embedded in the potential of the external atoms in the crystal. The latter is obtained by generating the atomic electronic density at the sites of several shells of atoms external to the cluster, with numerical atomic LSD calculations. The embedding potential is improved by performing self-consistent field (SCF) atomic calculations for the external atoms, with atomic populations similar to those obtained for atoms in the cluster. The Madelung potential of the crystal is included through the method of Ewald. Localization of cluster orbitals due to the Pauli exclusion principle is simulated by truncation of the potential of the external atoms at the core region [23]. In figure 1 a view of the cluster is depicted. A Y atom is placed at the centre of the cluster,

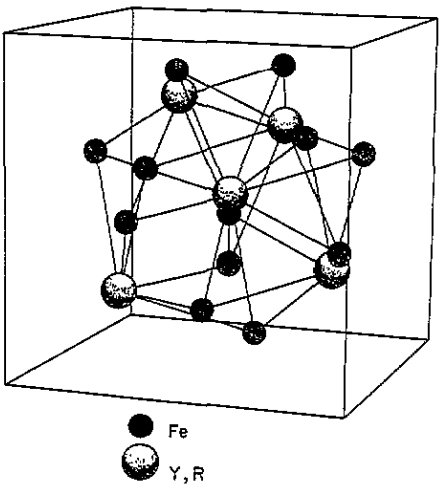

Figure 1. A view of the cluster representing Laves-phase compounds. A Y atom is at the centre.

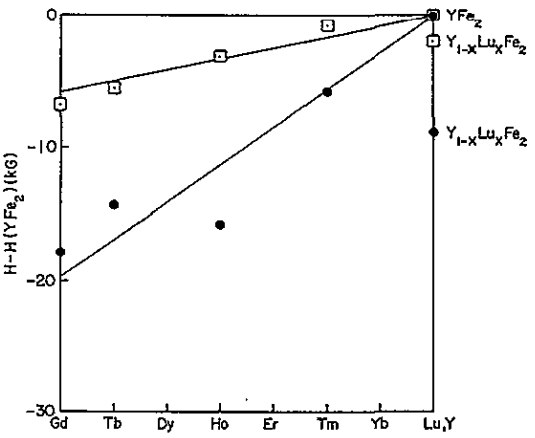

Figure 2. Components of the HF field at the central Y atom in mono-substituted clusters $[YFe_{12}(RY_3)]$ representing $Y_{1-x}R_xFe_2$, after subtraction of the value for YFe_2: ⊡, dipolar field H_D; ●, Fermi or contact field H_c. The lines drawn are to guide the eye.

since the atom at this position will be better described, being surrounded by two shells of neighbours.

In the DVM, the one-particle Kohn–Sham equations [24] are solved (in Hartrees):

$$(h_\sigma - \epsilon_{i\sigma})\phi_{i\sigma} = (-\nabla^2/2 + V_c + V_{xc}^\sigma - \epsilon_{i\sigma})\phi_{i\sigma} = 0 \tag{1}$$

where the Coulomb potential V_c includes inter-electronic repulsion and the electron–nuclear attraction; V_{xc}^σ is the exchange–correlation potential and depends on the spin σ. In the present calculation, we have employed V_{xc}^σ as given by von Barth and Hedin [25], which is, as the Coulomb potential, a functional of the electronic density associated with each spin σ:

$$\rho_\sigma(r) = \sum_i n_{i\sigma}|\phi_{i\sigma}(r)|^2 \tag{2}$$

where $n_{i\sigma}$ is the occupation of spin-orbital $\phi_{i\sigma}$, determined by Fermi–Dirac statistics. In a spin-polarized computation, $\rho_\uparrow$ may be different from $\rho_\downarrow$. The spin-orbitals of the clusters are linear expansions (LCAOs) on a basis of numerical symmetrized atomic orbitals $\{\chi_j^s\}$:

$$\phi_{i\sigma}(r) = \sum_j \chi_j^s(r)C_{ij}^\sigma. \tag{3}$$

The application of the variational method in a discrete grid of points leads to the secular equations

$$(\mathbf{H} - \mathbf{ES})\mathbf{C} = 0 \tag{4}$$

where **H** is the Hamiltonian matrix, **E** the eigenvalue matrix, **C** is the matrix of eigenvectors and **S** the overlap matrix. All the matrix elements are computed numerically in the

tridimensional grid of points. Iterations are made until the set $\{\phi_{i\sigma}\}$ is self-consistent with the potential, within a prescribed accuracy. For the present calculations, electronic charges and moments were converged up to $\pm 0.02e$ and $\pm 0.02\mu_B$ respectively. To define magnetic moments, the concept of Mulliken populations [26], which is based on the coefficients of the LCAO expansion, is adopted. The magnetic moments on the atoms are defined as the difference between the total Mulliken populations [26] for spin up and spin down.

In the variational expansion of the cluster spin-orbitals $\phi_{i\sigma}$, all atomic orbitals are included for the central Y atom, for which the hyperfine interactions were calculated. For Fe and Ni, only the 3d, 4s and 4p were kept in the variational basis, the others being kept frozen in the core and orthogonal to the valence. For the other Y atoms and for the lanthanides, the valence orbitals and the 'shallow core' orbitals (4s and 4p for Y, 5s and 5p for R) were included in the variational space. Atomic basis functions were obtained numerically by LSD calculations, and were optimized in further iterations by considering orbitals populations as obtained for the clusters. In these calculations, we considered it important to include the 4f orbitals of the lanthanides in the valence; this led to problems of convergence, which were circumvented by inducing fractional occupations of the levels near the Fermi level by a 'thermal distribution' sufficiently broad to allow convergence. This procedure led to a small degree of artificial occupation of the minority spin bands placed around the Fermi level.

In the DVM, a model potential is employed, constructed from multipolar expansions of the electronic charge density around each atomic site [27]. This expansion may be carried to any degree of accuracy; for the present compact solids, we considered it sufficient to include only overlapping spherical terms. In fact, the mean square error of the fit to the true density was of the order of $10^{-2}e/a_0^3$.

The tridimensional grid employed in the DVM is divided in two regions. In a spherical volume around each nucleus where a more precise numerical integration is needed, a regular grid of points is defined [28]. In the present calculations, this was done for the central Y atom, where the HF field was calculated, and for the rare-earth atoms, where higher numerical precision was found to be necessary. In all other regions of space, the grid points are pseudo-random Diophantine [10, 11], induced to be more dense near the nuclei. A total of $\sim 23\,000$ points was employed for the cluster integration grid.

The HF contact field (or Fermi field) computed at the Y nucleus, on the site (0, 0, 0) of the cluster, is given by

$$H_c = (8\pi/3)g\mu_B\tfrac{1}{2}[\rho_\uparrow(0) - \rho_\downarrow(0)] \tag{5}$$

where μ_B is the Bohr magneton, g the electronic g-factor and ρ is calculated according to (2). The elements H_D^{ij} of the dipolar HF tensor are given by

$$H_D^{ij} = \tfrac{1}{2}g\mu_B \int (\rho_\uparrow(r) - \rho_\downarrow(r)) \left(\frac{3x_i x_j - r^2\delta_{ij}}{r^5}\right) d\tau. \tag{6}$$

The orbital HF field at the Y site was assumed to be small due to quenching of the orbital angular momentum in the metallic environment, and was neglected. Therefore, the total HF field H_F is given by

$$H_F \cong H_C + H_D. \tag{7}$$

3. Analysis of the experimental data

The transferred HF fields at the Y site, in the pseudo-binary intermetallic compounds of formula $(Y_{1-x}R_x)Fe_2$ (with $x = 0.02$), were measured by zero-field spin echo NMR of ^{89}Y [20]. The samples of the pseudo-binary compounds were prepared by melting the high-purity constituents in an arc furnace, and were studied at 4.2 K.

The HF fields were obtained from the least-squares analysis of the NMR spectra. Each configuration of rare-earth second neighbours gives rise to a line in the spectrum, and the corresponding HF fields were obtained. The configurations are identified by their *probability of occurrence, at the concentration of the compound examined, assuming* a random occupation of the rare-earth sites by the impurities. In the computer fits, the line intensities are taken as proportional to these probabilities. The results reported in the present work were obtained from a configuration characterized by one single R neighbour near the Y probe atom.

4. Theoretical results and discussion

All the clusters chosen, representing a Y atom and its immediate environment in the crystal, have Y at the centre, surrounded by a shell of 12 transition-metal atom nearest neighbours (NNs) and by four Y or R atoms as next-nearest neighbours (NNNs) (see figure 1). In the clusters, the Y atom at the centre is best described, since all its chemical bonds are saturated. The pure compounds are thus represented by the clusters $[YFe_{12}Y_4]$ and $[YNi_{12}Y_4]$; the configurations with only one lanthanide atom substituting for Y in the NNN shell is represented by the clusters $[YFe_{12}(RY_3)]$ and $[YNi_{12}(RY_3)]$. The locally R-concentrated configurations are described by the clusters $[YFe_{12}R_4]$ and $[YNi_{12}R_4]$. In the case of the Fe compound, several rare earths were included (R = Gd, Tb, Ho, Tm or Lu), since we were looking for trends among the heavier lanthanides. For the Ni pseudo-binary compounds, only Gd was considered. All the clusters were embedded in the potential of several shells of atoms of the pure crystals. In the latter, each Y atom is surrounded by alternating shells of Fe (or Ni) and Y. The total charge on the clusters was determined self-consistently, by assuming in each iteration the Y charge as for the central atom, taking into account the stoichiometry [29].

Charge transfer is observed from Y (or R) to Fe or Ni, consistent with the higher Pauling eletronegativities of the transition metals [30]. Employing a definition in which the charge density $\rho(r)$ is distributed among the atoms according to the proximity of the point r to *their nuclei, we obtain, by integration of* ρ, *charges of* $\sim +0.8$ *on* Y; *values on* R *are* similar.

The calculated spin magnetic moments for YFe_2 are $-0.19\mu_B$ for Y_c and $1.39\mu_B$ for Fe. The large 3d magnetic moments of Fe are defined as positive by convention (majority spin up), here and elsewhere in this paper. Thus, the Y moments are aligned antiferromagnetically to Fe. For Y_p the moments are slightly smaller, since they are induced by hybridization and for these atoms the bonds are partly truncated. The total amount per formula unit is $2.65\mu_B$. *Experimental results point to somewhat higher values:* $2.90\mu_B$ for YFe_2 *from* magnetometry measurements [31] and $-0.67\mu_B$ on Y estimated from polarized neutron diffraction, of which 20% is believed to be the orbital moment contribution [2]. Theoretical values of the spin moment for Y range from $-0.29\mu_B$ from a tight-binding calculation [4] to $-0.38\mu_B$ [6] and $-0.43\mu_B$ [32] with the local-density LMTO method, and $-0.45\mu_B$ with the local-density ASW (augmented spherical wave) method [5]. As described in section 2, the

fractional electron distribution utlized to faciliate convergence has the effect of somewhat underestimating magnetic effects in the clusters, so our calculated values should be regarded more as trends among the different compounds. The calculated magnetic moment on Y_c is a sum of the 4d moment ($-0.15\mu_B$) and a small contribution from the conduction electrons with the same sign ($-0.04\mu_B$).

The contact HF field H_c at the Y atom in YFe_2, calculated at Y_c with the use of (5) is -154 kG, also somewhat underestimated as compared to the experimental value, -222 kG [21]. (Consistent with the convention adopted for the magnetic moments, the negative values of the HF fields at the Y nucleus signify that the majority spin density at the Y nucleus is constituted of spin-down electrons, here and elsewhere in this paper. In other words, the s electrons at the Y site are polarized antiferromagnetically relative to the positive magnetic moments at the Fe atoms.) Therefore, values for the R-substituted compounds will be presented relative to this value, i.e., after subtraction of the value for YFe_2. Due to the local tetrahedral symmetry around Y in YFe_2, the dipolar component H_D of the field vanishes. In the Y contact field, in contrast to Fe, the valence contribution (5s) is by far the dominant one.

In figure 2 the calculated values of the contact field H_c (after subtraction of the value for YFe_2), and the dipolar field H_D at the Y_c site of the clusters $[YFe_{12}(RY_3)]$, are plotted. The dipolar fields are created at the Y site by the spin-density asymmetry produced by the presence of one rare-earth NNN atom. To calculate H_D, the direction of magnetization taken into account was (1, 1, 1), which is the direction in YFe_2 and dilute $Y_{1-x}R_xFe_2$ [1]. For one R impurity in this direction (see figure 1) this is actually the direction in which the tensor of components H_D^{ij} is diagonal. It is seen that the variation of H_D is almost linear with Z; this is not the case with H_c. Although Lu has a zero 4f spin moment, its effect on the NNN Y atom is not the same as that produced by a Y atom in the same position, resulting in lower HF fields. These results show that, although the dipolar fields are much smaller than the total contact fields ($|H_D| \sim 2$–5 kG, $|H_c| \sim 200$ kG), the former make an important contribution to the *trend* of the HF fields for the different R-impurity systems.

In figure 3 the values of $H_F = H_c + H_D$ for the clusters with four NNN substitutions are compared to those with one substitution. The clusters $[YFe_{12}R_4]$ also present local tetrahedral symmetry around Y_c; consequently the dipolar field vanishes and the only component considered is H_c. For the locally R-concentrated case, the dependence of H_F on Z of the lanthanide is much more clear-cut than for only one substituent. The trends presented for the two cases in figure 3 show clearly that the increase in H_F is not linear in the number of R substituents, rather reaching a saturation value. In fact, the values of H_F for four R NNNs (the maximum number, see figure 1) are far from being four times larger than those for one R neighbour. This is due in part to the dipolar field, present only in the low-symmetry configuration. However, even the transferred contact fields do not increase linearly with the number of R neighbours: this may be seen clearly when comparing H_c in figure 2 (one neighbour) with H_c in figure 3 (four neighbours).

In figure 4 the calculated values of $H_F = H_c + H_D$ for the configuration with one R substituent are compared to the experimental values, obtained from measured data with the analysis described in section 3. Although the trends are similar in both cases, the variation is steeper for the calculated values. This discrepancy suggests that the orbital contribution to the hyperfine field at the Y atom may be non-negligible. This hypothesis is plausible since neutron-diffraction measurements on YFe_2 indicate the presence of an orbital moment on Y [2]. Orbital HF fields could be positive [33] and their inclusion in the calculation could decrease the absolute values of the fields; they may also be sensitive to the R substitutents. Calculation of orbital fields, however, is beyond the scope of this work.

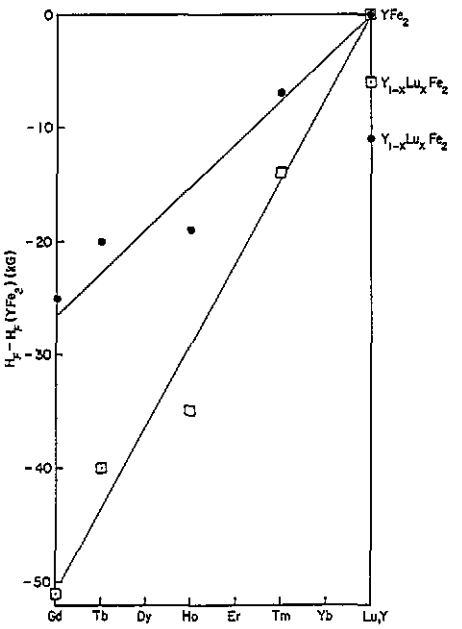

Figure 3. Sum of the dipolar and contact fields ($H_F = H_D + H_c$) at the central Y atom in clusters representing $Y_{1-x}R_xFe_2$, *after subtraction of the value for* YFe_2: ● one NNN substitution ($[YFe_{12}(RY_3)]$); ⊡, four NNN substitutions ($[YFe_{12}R_4]$). The lines drawn are to guide the eye.

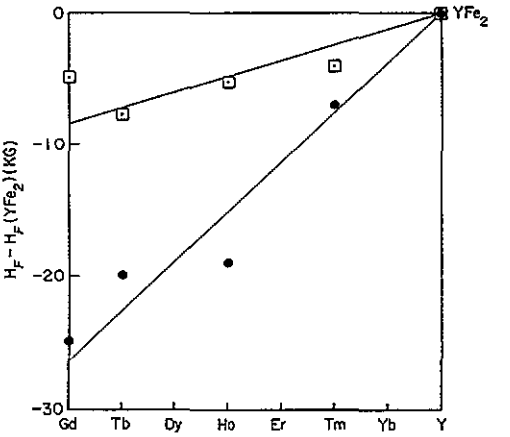

Figure 4. Experimental (⊡) and total calculated (●) HF fields at the Y site in compounds $Y_{1-x}R_xFe_2$ *for configurations with one NNN substitution, after* subtraction of the value for YFe_2. Calculated values ($H_F = H_D + H_c$) were obtained at Y_c for clusters $[YFe_{12}(RY_3)]$. The lines drawn are to guide the eye.

The variations observed in the Y HF fields along the series of lanthanides are clearly related to the different spin magnetic moments of R. The average transferred HF field in concentrated metallic systems has been observed to be broadly proportional to the spin of R in the compounds RFe_2 and R_2Fe_{17} [1, 34] and in R_xHo_{1-x} binary alloys [35]. The local HF field near a rare-earth impurity is also expected to be roughly proportional to the spin of the rare earth [35]. Accordingly, one may expect a decrease of the magnitude of the HF field at the Y site, as the rare-earth NNN is varied from Gd to Y or Lu. The mechanism through which this takes place is not obvious. Magnetic polarization in metals is thought to propagate by the mediation of the conduction electrons (RKKY mechanism) [1] or by direct, localized d–d hybridization [36]. The situation here is even more complex, since we are dealing with the influence of R on second-neighbour atoms.

First-principles band-structure calculations for YFe_2 have shown that the observed pressure dependence of the Y HF field is due to the fact that this field originates from the polarization of the s conduction electrons by the Fe (3d) magnetic moments [37]. In the case of the lanthanides, the 4f spin moments polarize the 5d electrons; these in turn may hybridize with the d electrons of Fe and Y. One question which poses itself is whether the transferred HF contact fields H_c on Y originate from increased 4d magnetic moments on Y, or from direct polarization of the s cloud by the R 4f and 5d electrons. To answer this question, we have plotted in figure 5 the 5d spin magnetic moments of the rare earths investigated, together with the Y_c magnetic moments, calculated for the clusters $[YFe_{12}(RY_3)]$. In figure 5, the R 5d moments are divided by μ(4d) of Y_p in YFe_2 and the Y 4d moments are divided by μ(4d) of Y_c in YFe_2. It is seen from the figure that μ(5d)

Table 1. Magnetic moments and HF fields in clusters representing Gd-substituted YNi_2.

Compound	Cluster	$\mu(4d)$ (μ_B)	H_D (kG)	H_c (kG)	$H_F = H_D + H_c$ (kG)
$Y_{1-x}Gd_xNi_2$	$[YNi_{12}(GdY_3)]$	0.00	−6.2	−12.7	−19
	$[YNi_{12}Gd_4]$	−0.01	—	−48.0	−48

varies significantly with Z of the lanthanide, and thus with the 4f moments of R (calculated $\mu(4f)$ are slightly lower than the free-atom values, due mainly to some intra-atomic 5d→4f charge transfer, which occurs mainly into the minority-spin 4f levels; the values are Gd, −6.4; Tb, −5.3; Ho, −3.1; Tm, −0.4). The Y magnetic moments, however, remain almost constant along the series. Therefore, we may conclude that variations in H_c at Y due to different R substituents are not due to changes in $\mu(4d)$ on the Y, but to direct polarization of the conduction electrons by the 4f and 5d electrons of R. The negligible changes in $\mu(4d)$ of Y are readily understood when one realizes that d–d interactions are short range, while R and Y are second neighbours.

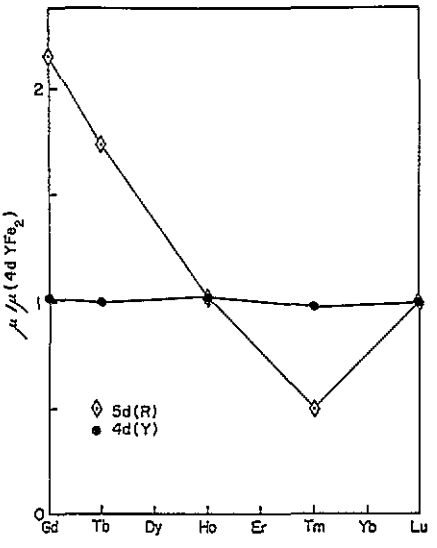

Figure 5. Ratios of calculated magnetic moments for $[YFe_{12}(RY_3)]$ clusters, representing $Y_{1-x}R_xFe_2$ compounds with one NNN substitution. The lines drawn are to guide the eye.

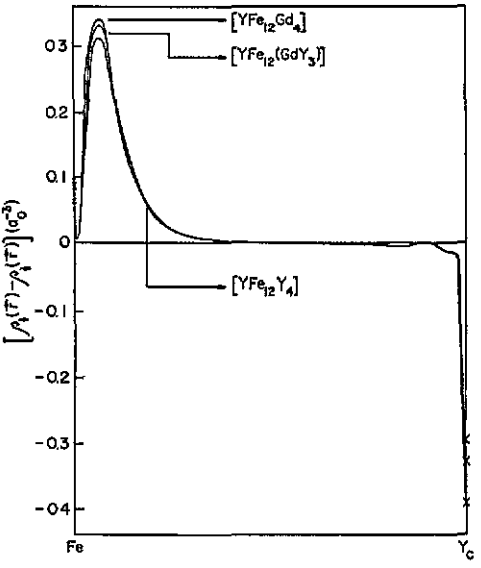

Figure 6. Valence spin density along the Fe–Y_c direction for $[YFe_{12}Y_4]$, $[YFe_{12}(GdY_3)]$ and $[YFe_{12}Gd_4]$. In the case of $[YFe_{12}(GdY_3)]$, the Fe atom is NN to Gd. For Y, 4s and 4p orbitals are also included.

It should be pointed out that the variation of $\mu(5d)$ on R along the series is steeper than that found in RFe_2 compounds by band structure calculations with the LMTO method [38].

In figure 5, it is seen that $Y_{1-x}Lu_xFe_2$ does not follow the trend of the other rare-earth-substituted compounds, presenting an increased $\mu(5d)$ with respect to $Y_{1-x}Tm_xFe_2$. This was seen to result from intra-atomic 5d→4f charge transfer: since this cannot take place in Lu, due to the completely filled 4f shell, the 5d population is increased (for both spins), and consequently, so is $\mu(5d)$.

The spin polarization produced by R is also extended to the Fe atoms. This is observed in figure 6, where the valence spin density $[\rho_\uparrow(r) - \rho_\downarrow(r)]$ is plotted in the Fe–Y_c direction for YFe_2 and $Y_{1-x}Gd_xFe_2$ with one and four NNN Gd atoms.

Further insight on the origin of the HF fields is gained by analysing pure and R-substituted YNi_2. YNi_2 is known to be non-magnetic [1]; indeed, a self-consistent calculation initiated with a rather large magnetic moment on Ni converges fully to the paramagnetic solution. In this case, therefore, the influence of R may be seen without the additional complication of the transition-metal magnetism. In table 1 results are shown for Gd-substituted YNi_2. It is seen that, although the spin magnetic moment on Y is negligible, non-negligible values of the dipolar field H_D and contact field H_c are obtained on Y. The values found are similar to differences in H_D and H_c values between YFe_2 and $Y_{1-x}Gd_xFe_2$, showing that in the latter roughly the same polarization is superposed to that induced by Fe. Another interesting feature is the 37% reduction of μ(5d) of Gd in $[YNi_{12}(GdY_3)]$, relative to μ(5d) of Gd in $[YFe_{12}(GdY_3)]$, showing that the 3d moment of Fe also contributes to polarize the 5d orbital of Gd.

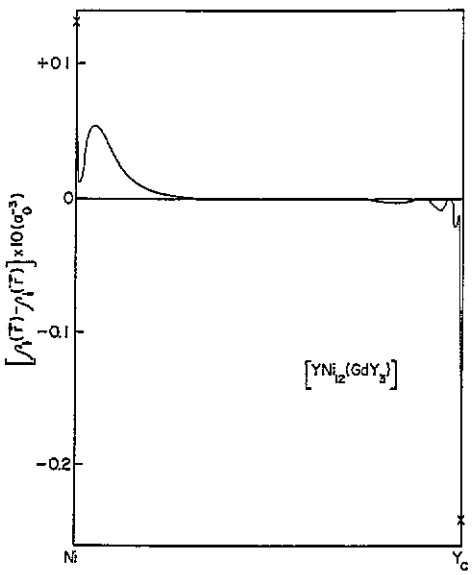

Figure 7. Valence spin density along the Ni–Y_c direction for $[YNi_{12}(GdY_3)]$. The Ni atom is NN to Gd.

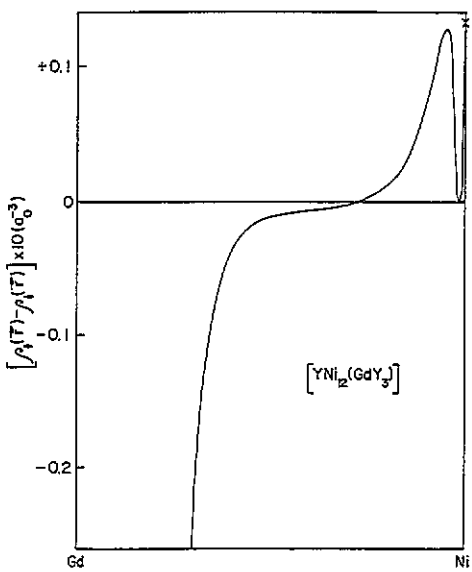

Figure 8. Valence spin density along the Gd–Ni direction for $[YNi_{12}(GdY_3)]$.

In figures 7 and 8 the valence spin density in $[YNi_{12}(GdY_3)]$, in the Ni–Y_c and Gd–Ni directions, respectively, is displayed. The polarization induced by Gd extends over Y and Ni; in the latter, we may also see an induced polarization of the 3d orbital, which is clearly larger in the Ni–Gd direction.

5. Conclusions

Through self-consistent local spin-density calculations for clusters representing a Y atom and its vicinity in $Y_{1-x}R_xFe_2$ and $Y_{1-x}R_xNi_2$, we have gained understanding of the mechanisms related to transferred hyperfine fields. The dipolar HF field induced by one NNN rare-earth neighbour is seen to increase significantly in the series Y, Lu $\rightarrow$ Gd; the variation obtained is almost linear. The transferred contact field at the Y site is seen to originate from direct polarization of the conduction electrons by the 4f and 5d electrons on the rare earth, and not from increased μ(4d) on Y.

Acknowledgments

The authors are grateful to Rio Data Centro, the computing centre of the Catholic University of Rio de Janeiro, for giving access to their IBM 9121 computer, where these calculations were performed. Thanks are also due to A A Gomes for several fruitful discussions.

References

[1] Buschow K H J 1977 *Rep. Prog. Phys.* **40** 1179
[2] Ritter C 1989 *J. Phys.: Condens. Matter* **1** 2765
[3] Armitage J G M, Dumelow T, Riedi P C and Abell J S 1989 *J. Phys.: Condens. Matter* **1** 3987
[4] Yamada H, Inoue J, Terao K, Kanda S and Shimizu M 1984 *J. Phys. F: Met. Phys.* **14** 1943
[5] Mohn P and Schwarz K 1985 *Physica* B **130** 26
[6] Eriksson O and Svane A 1989 *J. Phys.: Condens. Matter* **1** 1589
[7] Oppelt A and Buschow K H J 1973 *J. Phys. F: Met. Phys.* **3** L212
[8] Riedi P C and Webber G D 1983 *J. Phys. F: Met. Phys.* **13** 1057
[9] Alves K M B, Alves N, Guimarães A P, Mackenzie I S and Ross J W 1986 *J. Magn. Magn. Mater.* **54–7** 501
[10] Ellis D E 1968 *Int. J. Quantum Chem.* S **2** 35
[11] Ellis D E and Painter G S 1970 *Phys. Rev.* B **2** 2887
[12] Guenzburger D and Ellis D E 1987 *Phys. Rev.* B **36** 6971
[13] Guenzburger D, Ellis D E and Danon J 1986 *J. Magn. Magn. Mater.* **59** 139
[14] Chacham H, Galvão da Silva E, Guenzburger D and Ellis D E 1987 *Phys. Rev.* B **35** 1602
[15] Guenzburger D and Ellis D E 1991 *Phys. Rev. Lett.* **67** 3832
[16] Guenzburger D and Ellis D E 1992 *Phys. Rev.* B **45** 285
[17] Guenzburger D and Ellis D E 1985 *Phys. Rev.* B **31** 93
[18] Ellis D E and Guenzburger D 1985 *Phys. Rev.* B **31** 1514
[19] Alves K M B, Alves N, Sampaio L C, Cunha S F and Guimarães A P 1990 *J. Appl. Phys.* **67** 5867
[20] Alves K M B and Guimarães A P 1991 *J. Appl. Phys.* **70** 7632
[21] Oppelt A and Buschow K H J 1976 *Phys. Rev.* B **13** 4698
[22] Parr R G and Yang W 1989 *Density Functional Theory of Atoms and Molecules* (New York: Oxford University Press)
[23] Ellis D E, Benesch G A and Byron E 1977 *Phys. Rev.* B **16** 3308
[24] Kohn W and Sham L J 1965 *Phys. Rev.* A **140** 1133
[25] von Barth U and Hedin L 1972 *J. Phys. C: Solid State Phys.* **5** 1629
[26] Mulliken R S 1949 *J. Chem. Phys.* **46** 479
[27] Delley B and Ellis D E 1982 *J. Chem. Phys.* **76** 1949
[28] Stroud A H 1971 *Approximate Calculation of Multiple Integrals* (Englewood Cliffs, NJ: Prentice Hall)
[29] Terra J and Guenzburger D 1991 *Phys. Rev.* B **44** 8584
[30] Shriver D F, Atkins P W and Lanford C H 1990 *Inorganic Chemistry* (New York: Freeman)
[31] Buschow K H J and van Stapele R P 1970 *J. Appl. Phys.* **41** 4066
[32] Eriksson O, Johansson B, Brooks M S S and Skriver H L 1989 *Phys. Rev.* B **40** 9519
[33] Ebert H, Zeller R, Drittler B and Dederichs P H 1990 *J. Appl. Phys.* **67** 4576 and references therein
[34] Guimarães A P and Bunbury D St P 1973 *J. Phys. F: Met. Phys.* **3** 885
[35] McCausland M A H and Mackenzie I S 1979 *Adv. Phys.* **28** 305
[36] Campbell I A 1972 *J. Phys. F: Met. Phys.* **2** L47
[37] Dumelow T, Riedi P C, Mohn P, Schwarz K and Yamada Y 1986 *J. Magn. Magn. Mater.* **54–7** 1081
[38] Brooks M S S, Nordström L and Johansson B 1991 *J. Appl. Phys.* **69** 5683